Heliyon 10 (2024) e38091

Contents lists available at ScienceDirect

Heliyon

journal homepage: www.cell.com/heliyon

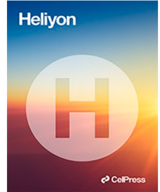

Research article

Landscape of epithelial cell subpopulations in the human esophageal squamous cell carcinoma microenvironment

Jingrong Yang [a,b,1], Bo Wu [b,c,1], Guo Li [a,b], Chenxi Zhang [a,b], Yongwei Xie [a,b], Wencui Kong [b,d,**], Zhiyong Zeng [a,b,*]

[a] Department of Cardiothoracic Surgery, The 900th Hospital of Joint Logistic Support Force, PLA, Fuzhou, 350025, China
[b] Fuzong Clinical Medical College of Fujian Medical University, Fuzhou, 350122, China
[c] Department of Emergency, The 900th Hospital of Joint Logistic Support Force, PLA, Fuzhou, 350025, China
[d] Department of Respiratory Medicine and Critical Care Medicine, The 900th Hospital of Joint Logistic Support Force, PLA, Fuzhou, 350025, China

A R T I C L E I N F O

Keywords:
Esophageal squamous cell carcinoma
Epithelial cells
Copy number variation
Pseudotime trajectory analysis
CellChat analysis
NK/T cells

A B S T R A C T

Aims: We sought to reveal the landscape of epithelial cell subpopulations in the human esophageal squamous cell carcinoma microenvironment and investigate their parts on esophageal squamous carcinoma (ESCC) development.
Background: Epithelial cells play an important role in the occurrence and development of ESCC through multiple mechanisms. While the landscape of epithelial cell subpopulations in ESCC, remains unclear.
Objective: Exploring the role of epithelial cell subpopulations in ESCC progression.
Methods: Seurat R package was used for single-cell RNA sequencing (scRNA-seq) data filtering, dimensionality reduction, clustering and differentially expressed genes analysis. Cellmarker database was adopted for cell cluster annotation. Functional enrichment analysis was carried out by Gene Ontology (GO) analysis. InferCNV package was conducted for copy number variation (CNV) of epithelial cell subpopulations in all chromosomal regions. Pseudotime trajectory analysis was implemented for exploring differentiation trajectory of epithelial cells subgroups during the cancer progression. CellChat analysis was used for probing the interactions between epithelial cells and NK/T cells. cellular experiments were performed using Quantitative Real-Time Polymerase Chain Reaction (RT-qPCR), Wound-Healing Assay and transwell.
Results: 11 major cell subpopulations were identified in ESCC and adjunct tissues. Further reclassification of epithelial cells uncovered 4 subpopulations. Enrichment analysis revealed that highly expressed genes in 4 epithelial cell subpopulations were related to cell proliferation, immune response and angiogenesis. CNV analysis found that UBD + epithelial cells and GAS2L3+ epithelial cells had a higher proportion of CNV. Cell differentiation trajectories disclosed that KRT6C+ and GSTA1+ epithelial cells were in an intermediate state of differentiation, while UBD+ and GAS2L3+ epithelial cells are in an end state of differentiation during ESCC progression. Finally, we found that four epithelial cell subpopulations all inhibited NK/T cells through NECTIN2-TIGIT and CLEC2B-KLRB1. Low ATF3 and DDIT3 mRNA expression inhibited ESCC cell migration and invasion.

* Corresponding author. Department of Cardiothoracic Surgery, The 900th Hospital of Joint Logistic Support Force, PLA, Fuzhou, 350025, China.
** Corresponding author. Fuzong Clinical Medical College of Fujian Medical University, Fuzhou, 350122, China.
E-mail addresses: kongwencui@163.com (W. Kong), 9201151059@fjmu.edu.cn (Z. Zeng).
[1] Equal Contribution.

https://doi.org/10.1016/j.heliyon.2024.e38091
Received 9 July 2024; Received in revised form 19 August 2024; Accepted 17 September 2024
Available online 18 September 2024
2405-8440/© 2024 The Authors. Published by Elsevier Ltd. This is an open access article under the CC BY-NC-ND license (http://creativecommons.org/licenses/by-nc-nd/4.0/).

Conclusion: Here, we obtained a through epithelial cell atlas of ESCC at single-cell resolution, explored the role of epithelial cell in ESCC progression, and unveiled immunosuppressive signals to NK/T cells in promoting ESCC. Our findings expand the comprehension of epithelial cells and offer a theoretical guidance for future anti-epithelial cell treatment of ESCC.

1. Introduction

Esophageal squamous cell carcinoma (ESCC) primarily develops in the upper and middle sections of the esophagus and represents one of the two principal forms of esophageal cancer [1,2]. According to cancer statistics from China, there were approximately 477, 900 new diagnoses of esophageal cancer, with an estimated 375,000 fatalities attributed to the disease in 2015 [3,4]. Owing to obscure symptoms, most ESCC patients are diagnosed as late stage. Surgery is the essential therapeutic methods in advanced stages (T2–T4 stages), accompanied with unfavorable life quality and inferior survival rate [5]. Recent clinical trials have also assessed molecular targeted therapies and immune checkpoint inhibitors for ESCC [6]. Cisplatin has served as a treatment option for ESCC and as a fundamental agent for both targeted therapy and immune checkpoint blockade in this cancer type [7]. However, resistance to the drug is another factor affecting the treatment of ESCC due to its significant toxicity and broad-spectrum antitumor activity. Greater than 70 % of patients with advanced disease do not achieve complete pathological remission after neoadjuvant drug chemotherapy and ultimately lead to tumor recurrence and poor prognosis [8]. To this end, a thorough understanding of molecular landscape of ESCC behind ESCC progression is of fundamental significance.

In the tumor microenvironment (TME), there are not only tumor cells, but also a large number of non-malignant cells, such as immune cells, epithelial cells and fibroblasts etc [9,10]. Abundant studies have shown that epithelial cells play an important role in the occurrence and development of ESCC. Zhang X et al. carried out single-cell RNA sequencing (scRNA-seq) in 60 ESCC individuals to probe the expression states varied within epithelial cells and deciphered 8 expression programs with distinct functions and cell status from malignant epithelial cells [11]. The finding indicates that the importance of epithelial cells in ESCC progression, because epithelial cells can promote the progress of ESCC through various mechanisms. In a recently published study, epithelial cell was uncovered to activate fibroblasts through ANXA1/FPR2 signaling to facilitate ESCC tumorigenesis [12]. In this regard, exploring of landscape of epithelial cell subpopulations had the prognostic value for ESCC.

Bulk sequencing analysis basing on large mixed tissues containing cancer cells and TME components, usually generates plentiful marker genes in multiple pathways. However, these marker genes cannot explain the dynamic state of various cells in heterogeneous tumor tissues and their interactions in cancer development. In this situation, scRNA-seq emerged [13]. This method allows massively parallel representation in thousands of cells, and can better interpret the crosstalk among cells. In recent years, some researchers have broadened the outlook into the collective communications of tumor cell in TME in ESCC by applying this technique [14–16]. While, relatively few studies have been published on the scRNA-seq study of epithelial cells in ESCC.

Here, we obtained scRNA-seq data from ESCC based on public databases. By identifying cellular subpopulations that have a strong influence on the development of ESCC, their potential biological functions, the presence of copy number variability, the identification of transcription factors, the evolution of cellular subpopulations, and the interactions between cells were analyzed and validated. These findings promote the comprehension of establishing a landscape of cell subpopulations in ESCC and propose a basis on refined targeting treatment directed toward tumor-facilitating epithelial cell subsets.

2. Material and methods

2.1. Data acquisition

GSE196756 [17] dataset containing scRNA-seq data of 3 paired specimens was enrolled from Gene Expression Omnibus (GEO) database. TCGA-ESCC cohort comprising expression profiles, mutational message and clinical information was downloaded from The Cancer Genome Atlas (TCGA).

2.2. scRNA-seq data filtering, dimensionality reduction, clustering, and annotation

The initial scRNA-seq data were inputted into the Seurat (v3.1.2) R package [18] for quality control and next analysis. All functions were executed with default parameters, unless explicitly stated otherwise. Low-quality cells (<200 or >10,000 genes and >10 % mitochondrial genes) were excluded. As a result, 28,585 cells were remained. Then the left cells were standardized using the SCTransform method. Harmony package was carried out to leach batch effects among different samples followed by Principal Component Analysis (PCA) dimensionality reduction. After Uniform Manifold Approximation and Projection (UMAP) dimensionality reduction, we constructed a KNN graph based on Euclidean distance adopting the FindNeighbors function. Subsequently, the FindCluster function was conducted for cell-clustering and sub-clustering analyses. The cell types were determined on the context of the specifically highly expressed marker genes known in the CellMarker database. The FindAllMarkers function was subjected to calculate the differentially expressed genes among each cell subgroup (average_logFoldchange >0.25 and p_value_adj <0.05).

2.3. Functional enrichment analysis

To further explore the biological functions in which the identified cell subpopulations may be involved, we uploaded specific gene collections into the DAVID database (http://david.abcc.ncifcrf.gov/). Next, based on the Gene Ontology (GO) enrichment analysis, the biological processes (BP) enriched by these gene collections were then observed.

2.4. Single cell copy number variation analysis

InferCNV R package [19] was conducted to characterize the initial copy number variation (CNV) of the epithelial cell subgroup in all chromosomal regions within the internal tumor tissue. Wherein, Plasma B cells were set as a reference [20]. The other parameter settings are as follows: cutoff = 0.1, cluster_by_groups = T, analysis_mode = "subclusters", HMM_type = "i3", denoise = T, HMM_report_by = "subcluster", HMM = T.

2.5. SCENIC analysis

SCENIC is a proper method for exploring transcription factors (TFs) to uncover cellular states from scRNA-seq data [21]. GENIE3 method was applied to calculate the potential target genes for each TF, and the top5 targets were used to establish a transcription factor regulatory network. Finally, we confirmed highly reliable TF target gene relationship pairs (regulons) and used the AUCell function to calculate the activity level of regulons within each cell.

2.6. Development of trajectory inference

To investigate the dynamic changes in gene expression of epithelial cells during the progression from normal to carcinogenic status, we performed single cell pseudotime trajectory analysis adopting R package monocle2 [22]. Detailed analysis process was as follows. We selected genes with an average expression value greater than 0.1 and expressed in at least 10 cells for subsequent analysis. The differentialGeneTest function was executed to select differentially expressed genes among epithelial cell subclusters with a parameter fullModelFormulaStr = "~cell_type". Based on above genes, the DDRTree algorithm was conducted to reduce dimensionality, and the orderCells function was adopted to sort the cells and complete trajectory construction based on the expression trend of highly variable genes. We used branches of cells containing adjacent cancer samples as the starting point for the differentiation trajectory. Cell division related genes (CDCA8, CDK6, DCTN1, MAEA and MAP4) and angiogenesis relevant genes (CALD1, CAV1, COL18A1, MMP2 and RBPJ) were also subjected to pseudotime trajectory analysis. Plot_pseudotime_heatmap function was used to describe the heatmap of gene expression levels changing with pseudotime.

2.7. CellChat analysis

CellChat, a tool which parses ligand-receptor action among cells, was carried out using the CellChat R package [23]. Here, we employed CellChat to investigate the ligand receptor pairs of epithelial cell subsets in tumor tissue that act on NK/T cells, and use bubble diagrams to display the possibility and significance of ligand receptor interactions among cell subsets.

2.8. Cell culture

The human-derived TE-1 cell lines (BNCC100151) and normal esophageal epithelial cell lines (HET-1A) were purchased from the BeNa Culture Collection. The TE- 1 cells were cultured in 1640 basal medium (Gibco, Waltham, MA, USA, Cat No: 8118131) supplemented with 10 % fetal bovine serum (FBS, Gibco, Waltham, MA, USA, Cat No: 42F7180K); the HET-1A cells were cultured in complete growth medium. The cells were cultured in a humidified atmosphere of 5 % CO_2 at 37 °C. TE-1 cells were transfected with small RNA using Lipofectamine 2000. siRNAs were purchased from GenePharma (Suzhou, China): 5′-GAUGAGAGAAACCUCUUUATT-3′ for ATF3; 5'-CCTGGAAATGAAGAGGAAGAA-3' for DDIT3; and 5′-UUCUCCGAACGUGUCACGUTT-3′ for scrambled siRNA (negative control).

2.9. Quantitative Real-Time Polymerase Chain Reaction (RT-qPCR)

Total RNA from cells was isolated using TRIzol reagent (Invitrogen) and were reverse transcribed into cDNA using the reverse transcription kit. The NovoStart SYBR qPCR SuperMix Plus (Novoprotein) was used for RT-qPCR analysis. The relative expression of

Table 1
Primers of genes.

Genes	Sense (5′–3′)	Anti-sense (5′–3′)
ATF3	CTGGAAAGTGTGAATGCTGAAC	ATTCTGAGCCCGGACAATAC
DDIT3	ACCTCCTGGAAATGAAGAGGAAG	CAGTCAGCCAAGCCAGAGAA
GAPDH	CAAGAGCACAAGAGGAAGAGAG	CTACATGGCAACTGTGAGGAG

gene in the cells was calculated according to the $2^{-\Delta\Delta Ct}$ formula using GAPDH as the internal reference. Primers of genes were listed in Table 1.

2.10. Wound-Healing Assay

TE-1 cells were seeded at 6×10^5 cells/well in a 6-well plate and for siRNA transfection in advance. Once the cell confluence

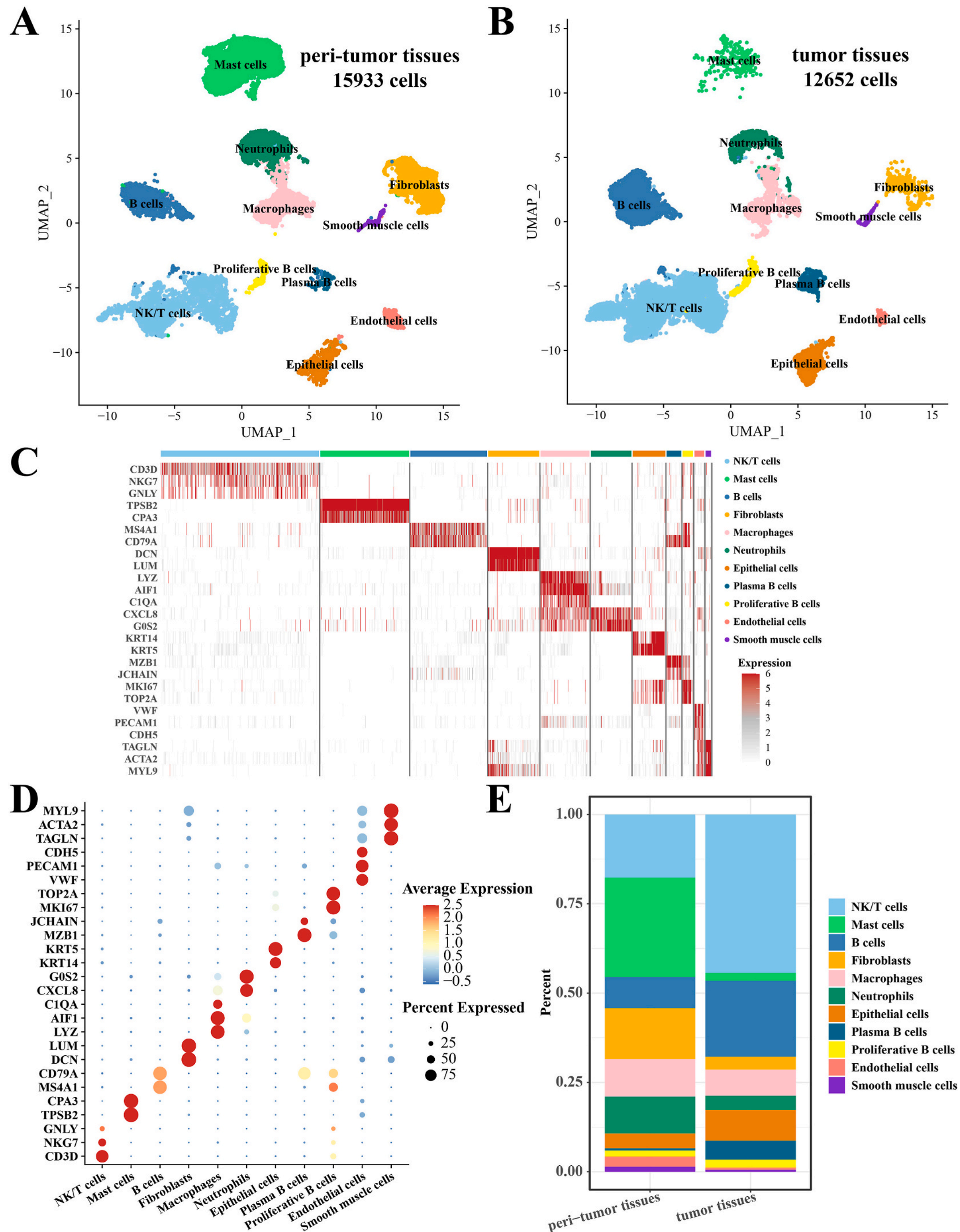

Fig. 1. Landscape of cell subpopulations in ESCC and adjacent tissues
(A, B) UMAP map of cell cluster annotation in adjacent and cancer tissues. (C, D) Marker gene expression in cell subpopulations described by a heat map or a bubble plot. (E) Bar chart showing the proportion of each cell subgroup in cancer and adjacent tissues.

reached 90 %, a wound area was carefully made in the cell monolayer with a sterile 200-μL pipette. The separated cells were washed with PBS. Cells migrated to the injured area and were observed under an Olympus CK-2 inverted microscope and photographed (100× magnification) at 0, and 48 h.

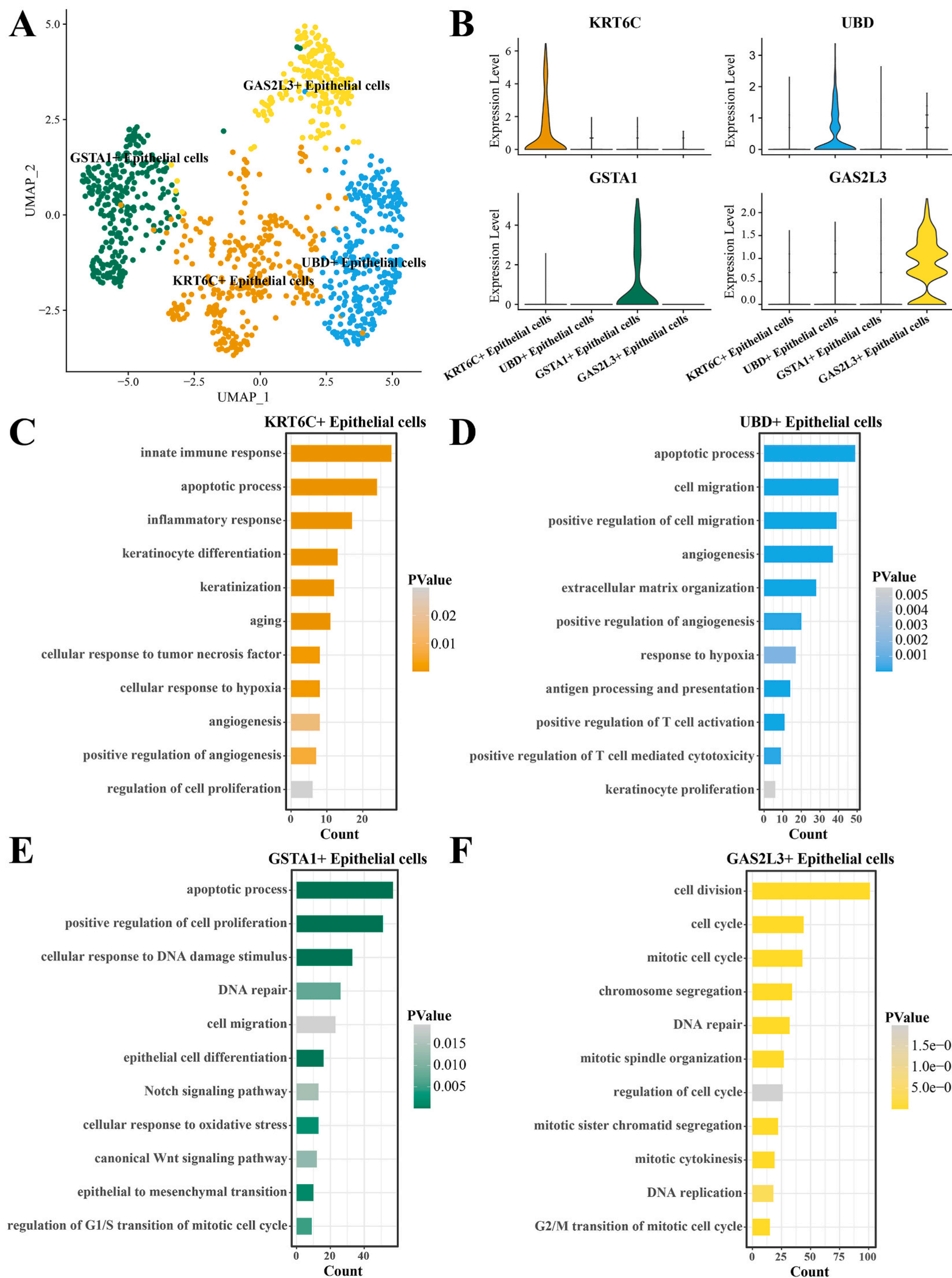

Fig. 2. Landscape of epithelial cell subclusters in ESCC specimens
(A) UMAP map of epithelial cell subclusters annotation in cancer tissues. (B) Marker gene expression in epithelial cell subclusters described by a violin plot. (C–F) Biological process enriched with highly expressed genes in each epithelial cell subcluster within cancer tissue (C) KRT6C + epithelial cells. (D)UBD + epithelial cells. (E)GSTA1+ epithelial cells. (F)GAS2L3+ epithelial cells.

2.11. Transwell assay

To evaluate the migratory capacity of TE-1 cells post-transfection, a Transwell migration assay was conducted. Specifically, 48 h after transfection in TE-1 cells, the cells in each group were collected by trypsinization and counted; 4×10^4 cells were added to 100 μL serum free medium and mixed, and then added to the bottom of the upper chamber of the Transwell chamber. The complete medium containing 10 % FBS was added to the lower chamber, and the apparatus was placed in an incubator for 48 h. The cells were then fixed with 4 % paraformaldehyde and stained with 0.1 % crystal violet staining solution. Micrographs were taken to count the number of cells that had penetrated the membrane.

2.12. Statistical analysis

All statistical analysis and figures were generated using R software (version 3.6.3). Two tailed wilcoxon rank sum test was applied to calculate the differences between two sets of continuous variables. The survival differences were depicted via Kaplan-Meier curves

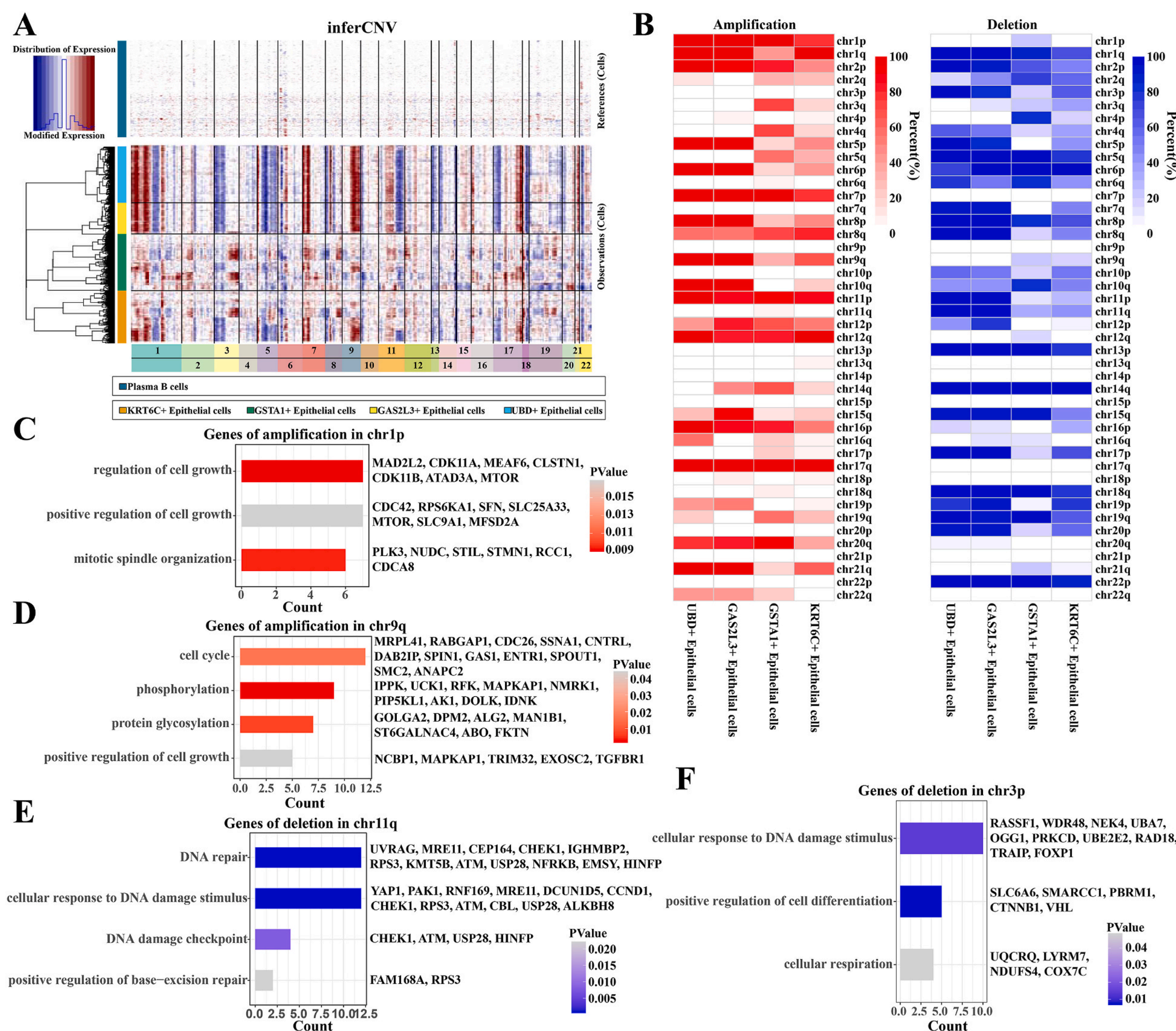

Fig. 3. CNV analysis of epithelial cell subclusters in ESCC tissues
(A) A hierarchical clustering heat map of CNV in four epithelial cell subsets. (B) A heat map describing the proportions of cells with expansion or deletion in each chromosome region of four epithelial cell subsets. Here, we roughly divided each chromosome into long arms and short arms. Color represented the proportions of cells with CNV events occurring within each subgroup. (C) Enriched biological processes of amplified genes in chr1p region. (D) Enriched biological processes of amplified genes in chr9q region. (E) Enriched biological processes of deleted genes in chr11q region. (F) Enriched biological processes of deleted genes in chr3p region. (For interpretation of the references to colour in this figure legend, the reader is referred to the Web version of this article.)

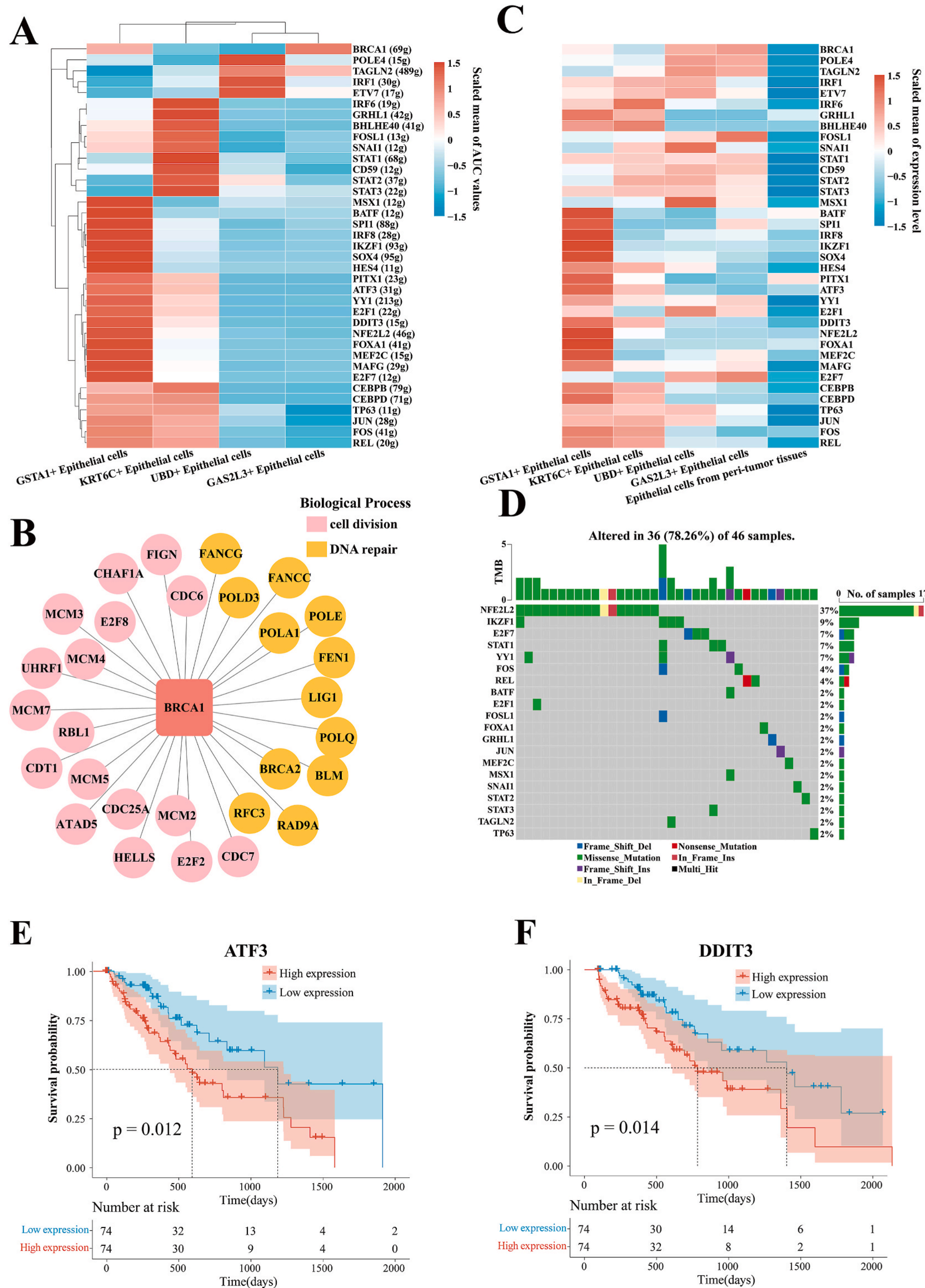

Fig. 4. SCENIC analysis of epithelial cell subsets
(A) A heat map of AUC values concerning regulons in four epithelial cell subpopulations in ESCC tissue. (B) A network diagram of genes related to BRCA1 regulating cell cycle and DNA repair. (C) A heat map describing TFs expression values of four epithelial cell subpopulations in ESCC tissues comparing with normal epithelial cells. (D) Waterfall plot of mutation spectrum about identified TFs in TCGA-ESCA cohort. (E, F) Survival curves of ATF3 and DDIT3 in TCGA-ESCA queue.

accompanied with log-rank test. Sangerbox (http://sangerbox.com/home.html) also offered auxiliary analysis in this paper [24]. A p-value <0.05 was considered statistically significant.

3. Results

3.1. Single cell atlas of ESCC and adjacent tissues

Through cell filtration, Peri-cancerous tissue reserved 15,933 cells, while cancer tissue reserved 12,652 cells (Fig. 1A and B). When resolution to 0.1was set for all cell clusters, 11 major cell subpopulations were identified (Fig. 1A and B). Via specifically highly expressed marker genes, we annotated these 11 cell cluster as NK/T cells (CD3D and NKG7) [25], mast cells (CPA3 and TPSB2) [26], B

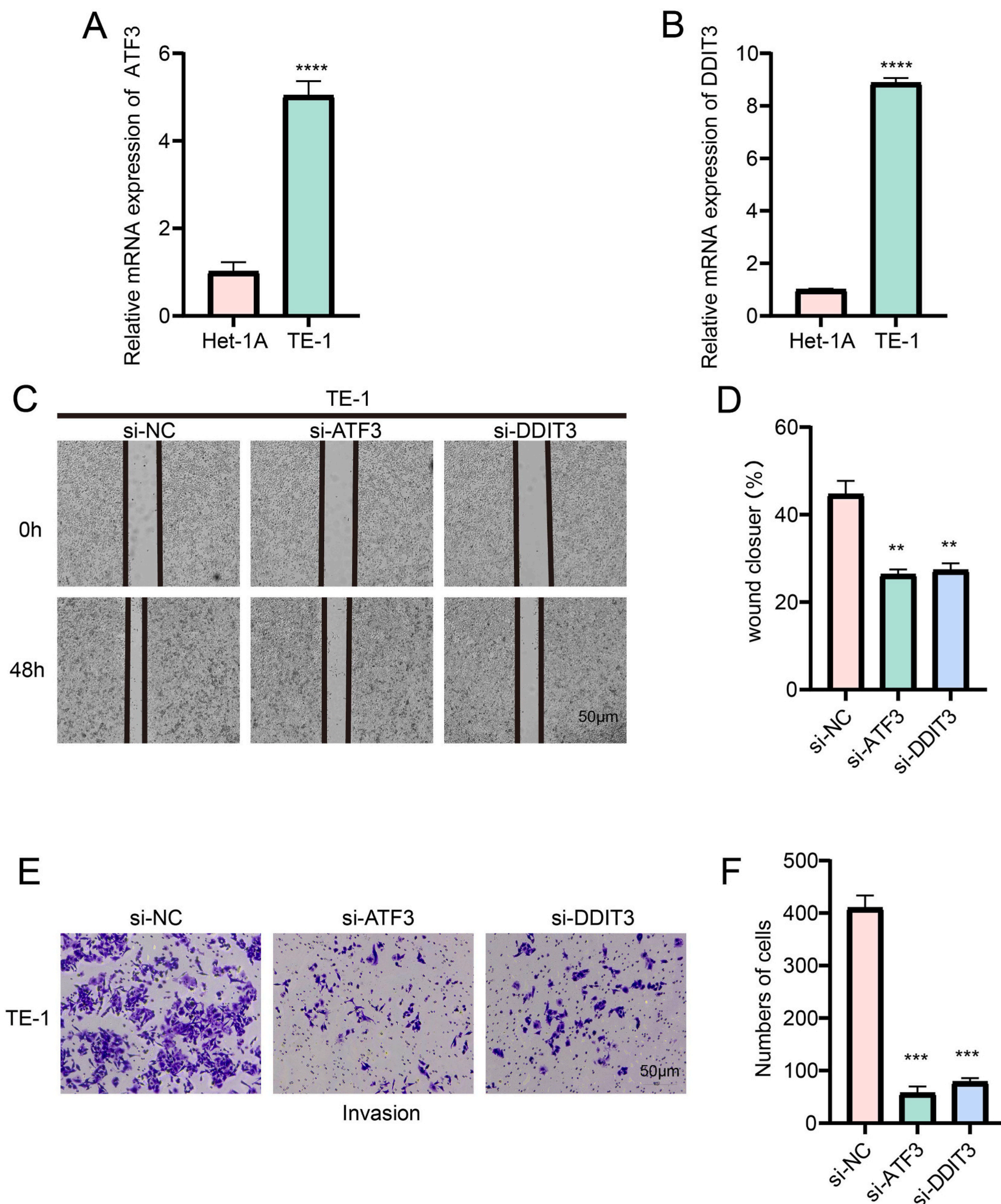

Fig. 5. ATF3 and DDIT3 higher expression promoted ESCC cell migration and invasion
(A) ATF3 was higher expression in ESCC cell line. (B) DDIT3 was higher expression in ESCC cell line. (C–D) Cell migration detected by the cell scratch test. (E–F) Cell migration detected by the Transwell assay. $^{**}p < 0.01$, $^{***}p < 0.001$, $^{****}p < 0.0001$.

cells (CD79A and MS4A1) [27,28], Fibroblasts (LUM and DCN) [29], Macrophages (LYZ, AIF1 and C1QA) [30,31], Neutrophils (G0S2 and CXCL8) [32], Epithelial cells (KRT5 and KRT14) [33], Plasma B cells (MZB1, JCHAIN and CD79A) [27,34], Proliferative B cells (TOP2A, MKI67, CD79A and MS4A1) [27,28], Endothelial cells (CDH5, PECAM1, VWF) [35], and Smooth muscle cells (MYL9, ACTA2, TAGLN) [36]. The marker genes of each cell cluster were depicted in a heatmap and a bubble chart (Fig. 1C and D). We further found that the proportions of NK/T cells, B cells, plasma B cells and epithelial cells in cancer tissue were higher, while the proportion of Mast cell, Macrophages, Neutrophils and Fibroblasts in peri-cancerous tissue were higher (Fig. 1E). Detailed information of 6 scRNA seq samples could be seen in Supplementary Fig. S1.

3.2. Diversity of endothelial cells in ESCC

Due to the crucial role of epithelial cells in the infinite proliferation of ESCC tissue [37], we extracted all epithelial cells from the cancer tissue and analyzed them again. Applying the same dimensionality reduction clustering method, epithelial cells were divided into four main cell subpopulations, and named with specifically highly expressed genes, when resolution to 0.2 was set for all cell clusters (Fig. 2A). The genes with specific high expression among different subpopulations were shown in Fig. 2B. To study the role of these four epithelial cell subpopulations in the occurrence and development of ESCC, we sequentially examined the biological processes enriched by their highly expressed genes (Fig. 2C–F). Interestingly, we found that KRT6C + epithelial cells were mainly related to the differentiation and keratinization of keratinocytes; UBD + epithelial cells were mainly connected with cell migration, antigen presentation and activation of T cells; GSTA1+ epithelial cells were correlated to DNA damage stimulation and repair, NOTCH signaling pathway and WNT signaling pathway. Specifically, GAS2L3+ epithellial cells were all enriched with cell division and cell cycle. These findings indicated that GAS2L3+ epithelial cells contributed most to the infinite proliferation of the entire tumor tissue. In addition, KRT6C + epithelial cells and UBD + epithelial cells were also associated with angiogenesis and hypoxic response, suggesting that these two cell subpopulations play a crucial role in angiogenesis, which in turn may influence tumor growth and immune escape.

3.3. CNV analysis of epithelial cell sub-clusters in ESCC tissues

The CNV results illuminated that the proportions of CNV were higher in UBD + GAS2L3+ epithelial cells. We could clearly observe that copy number amplification occurred in chr1p, chr7p, chr9q, and chr17q, while copy number deletion took place in chr3p, chr5, and chr11q (Fig. 3A). We also calculated the proportions of cells with expansion or deletion in each chromosome region for each epithelial cell subgroup, and found similar results (Fig. 3B). Specifically, we found that in the regions where chr1p and chr9q were amplified, there were many genes related to cell growth and cell cycle, such as MAD2L2, CDK11A and CDC26, etc. In addition, in the regions where chr3p and chr11q were deleted, there were many genes correlated with DNA damage repair, such as UVRAG, MRE11 and CHEK1, etc (Fig. 3C–F). These results implied that in ESCC epithelial cells, copy number amplification occurred in cell cycle related genes, while copy number deletion happened in DNA damage repair related genes.

3.4. Crucial TFs in epithelial cells of ESCC tissues

The AUC values of regulons in four epithelial cell subsets were exhibited in Fig. 4A. We detected that BRCA1 played an essential role in GAS2L3+ Epithelial cells, and further research unraveled that BRCA1 regulated many target genes related to cell division and DNA damage (Fig. 4B). POLE4, TAGLN2, IRF1 and ETV7 were involved in UBD + Epihelial cells. STAT1, STAT2, and STAT3 were more enriched in KRT6C + Epihelial cells. ATF3, E2F1, DDIT3 and NFE2L2 had a stronger participation in GSTA1+ Epithelial cells. In addition, the expression values of these TFs in epithelial cells of cancer tissue were higher than those in normal epithelial cells (Fig. 4C). The gene mutation analysis from TCGA-ESCA database proclaimed that NFE2L2 had the highest mutation frequency (Fig. 4D). The survival analysis hinted that only ATF3 and DDIT3 were closely associated with survival time in ESCC patients. The higher the expression value of these two TFs, the worse prognosis of the patients (Fig. 4E and F).

3.5. ATF3 and DDIT3 higher expression promoted ESCC cell migration and invasion

To explore the function of ATF3 and DDIT3 in ESCC malignant feature, RT-qPCR analysis showed that ATF3 and DDIT3 mRNA levels both upregulated in TE-1 cells in comparison to Het-1A (Fig. 5A and B). Moreover, Knockdown ATF3 and DDIT3 effectively inhibited TE-1 cells migration (Fig. 5C and D) and invasion (Fig. 5E and F). Those data implied that ATF3 and DDIT3 expressions maybe influence ESCC progression.

3.6. Evolutionary evolution of epithelial cell subclusters in the progression of ESCC

Pseudotime trajectory analysis was used to investigate the dynamic changes in gene expression of epithelial cells during the occurrence and development of esophageal cancer. We treated the branching of epithelial cells originating from adjacent cancer tissues as the starting point for the differentiation trajectory (Fig. 6A). As shown in Fig. 6B, KRT6C+ and GSTA1+ epithelial cells were located in the middle of the differentiation trajectory, while GAS2L3+ and UBD + epithelial cells were located at the end of the differentiation trajectory. This implied that KRT6C+ and GSTA1+ epithelial cells represented intermediate states during tumor development, while GAS2L3+ and UBD + epithelial cells stood for terminal states during tumor development. Further, we found that along with trajectory, the expression level of genes related to the positive regulation of cell division, angiogenesis, cell migration, and T cell activity gradually

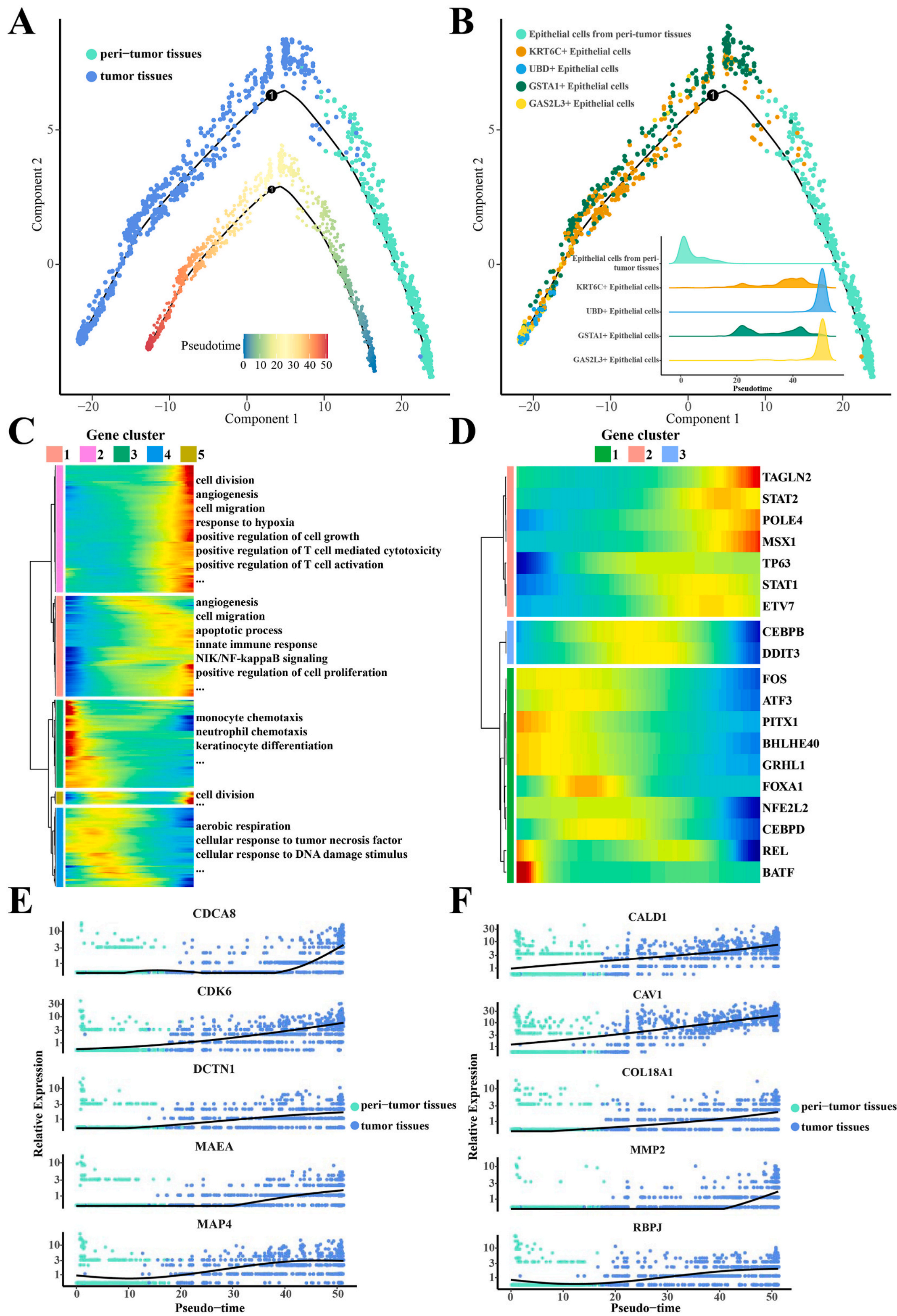

(caption on next page)

Fig. 6. Analysis of the differentiation trajectory on epithelial cells during the development of ESCC
(A) The differentiation trajectory of epithelial cell from peri-cancer to cancer state. (B) The distribution of each epithelial cell subgroups during the progression ESCC. (C) Changes in gene expression with pseudotime and corresponding enriched biological processes. (D) The varying expression of TFs identified in SCENIC analysis with pseudotime. (E) Scatter plot of the expression of cell division related genes with pseudotime changes. (F) Scatter plot of the expression of angiogenesis related genes with pseudotime changes.

increased, while the expression of genes related to aerobic respiration, tumor necrosis factor cell response, and DNA damage stimulated cell response gradually decreased (Fig. 6C). The expression levels of TFs such as TAGLN2, STAT2, and TP63 gradually raised with trajectory. Conversely, the expression levels of transcription factors such as FOS, ATF3, and PITX1 gradually declined with trajectory (Fig. 6D). The trend of changes in genes related to cell division and angiogenesis is shown in Fig. 6E and F.

3.7. ESCC epithelial cell subpopulations had inhibitory effects on NK/T cells

NK/T cells plays an important role in fighting cancer. A review uncovered that NK/T cells performed cancer immune surveillance by directly killing carcinogenic cells or coordinating the activity of anti-tumor immune cells [38]. Thereby, we explored the ligand

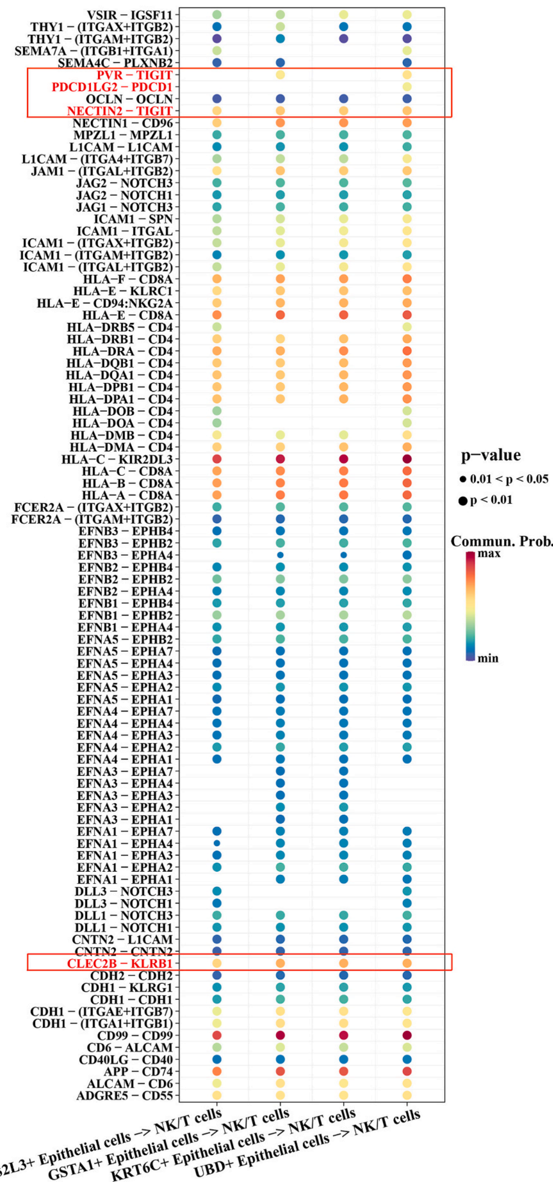

Fig. 7. A bubble diagram describing the direct interactions between epithelial cell subpopulations and NK/T cells via ligand-receptor pairs in ESCC.

receptor status of four epithelial cell subsets in ESCC tissues acting on NK/T cells. Since NK/T cells mainly killed tumor cells through direct contact, we chose the type of direct contact, and found that GSTA1+ and UBD + epithelial cells inhibited the activity of NK/T cells through PVR-TIGIT. Specifically, UBD + epithelial cells restrained the activity of NK/T cells through PDCD1LG2-PDCD1. Meanwhile, all epithelial cell subpopulations suppressed NK/T cell activity through NECTIN2-TIGIT and CLEC2B-KLRB1 (Fig. 7).

4. Discussion

The present studies on ESCC are mostly comprised of genomic and epigenetics studies, epidemiologic researches and clinical trials [39–43]. These studies extended our understanding on the existing treatment strategies for Esophageal cancer. Nevertheless, the prognosis of ESCC is still unsatisfying, with a five-year survival rate <20 % [44,45].As a consequence, precise exploration of the cellular heterogeneity of Esophageal cancer is in need. Currently, an in vitro animal model imitating human ESCC progression and descriptions on ESCC developmental atlas basing on scRNA sequencing have been published [37]. We integrated online scRNA-seq and CNV data to clarify the whole epithelial cell landscape, where different degrees of mutation and biological functions were identified, including the inhibitory effects on with immune NK/T cells.

The progression of ESCC require multiphase epithelial cancer formation, i.e., from normal epithelium, low and high degree intraepithelial neoplasia to invasive cancer [46]. More and more studies have explored the components or role of epithelial cells in the development of cancer. For instance, by means of E-cadherin cleavage from epithelial cells makes it possible for tumor cells to mechanically adapt to matrices with different stiffness [47]. In an in vitro experiment, Liu Y et al. proved that lung epithelial cells stimulate tumor extracellular RNA through Toll like receptor 3 (TLR3), which is essential for triggering neutrophil recruitment and lung premetastatic niche formation [48]. Epithelial cell was recently reported to activate fibroblasts through ANXA1/FPR2 signaling for contributing to ESCC tumorigenesis [12]. The literature mentioned above supported the noteworthy part of epithelial cells in ESCC development. Coherently, our preliminary single cell subpopulation atlas also found a higher proportion of epithelial cells apart from immunocytes in cancer tissue. Through subgroup cluster analysis, we identified a total of 4 epithelial cell subpopulations. Among them, UBD+ and GAS2L3+ Epithelial cells underwent a greater proportion of CNVs and amplification of chr1p, chr7p, chr9q and chr17q was observed to occur within this region. Bao et al. observed CNVs in several genomic regions including chr1p and chr9p in five breast cancer tissue samples and concluded that clonal amplification was observed in morphologically normal mammary epithelial cell regions, which may have been driven by a driver mutation and subsequent amplification of chr1q [49]. MAD2L2 serves as a novel regulator of cancer progression, which typically undergoes genomic alterations, including amplification and deep deletions [50]. Moreover, MAD2L2 expression has been reported to be associated with poor prognosis in patients with a variety of cancers, such as colon and ovarian cancers [50,51]. In particular, Diniz et al. demonstrated that the transcriptional activity of MAD2L2, one of the cell cycle-associated genes, is capable of varying according to tumor size in oral squamous cell carcinoma [52]. This is similar to our findings that the MAD2L2 gene was found to be significantly enriched in the region of chrp1 amplification in a pathway associated with the cell cycle. These results suggest that amplification of cell cycle genes occurs in ESCC, which in turn promotes tumorigenesis and progression.

Additionally, the pseudotime trajectory analysis revealed KRT6C+ and GSTA1+ epithelial cells may represent intermediate states, while GAS2L3+ and UBD + epithelial cells may represent terminal states during tumor development. The CNV results could also confirm this finding, as the proportions of CNV in GAS2L3+ epithelial cells and UBD + epithelial cells were greater. In the intermediate states of cancer progression, once the size of a tumor grows > 1–2 mm, it must set up separate vessel supply for oxygen and nutrients [53,54]. Angiogenesis, the process of forming new vascular tissues, is fundamental for tumorigenesis. Conversely, angiogenesis deficiency is believed to be a reason why some microscopic lesions do not develop into invasive cancer but keep dormant [55]. Hypoxia, insufficient oxygen in tissue, is a main incentive for angiogenesis [9]. Hypoxia-inducible factors has been reported to trigger the transcription of thousands of genes for angiogenesis [56]. In hypoxia environment, some signaling pathways such as Wnt signaling pathway and Notch signaling pathway are also activated for cancer cell proliferation as well as metastasis [57–59]. In the terminal states during tumor development, tumor needs to produce a large number of tumor cells for metastasis and diffusion [60]. The infinite proliferation ability of tumor tissue is particularly important in this process [61]. Interestingly, we carried out GO biological process analysis, and found that the enriched pathways of these 4 epithelial cell subpopulations corresponded to the process of cancer development. These results highlighted the importance of epithelial cell on ESCC growth. In addition, the major genes and TFs that differed in 4 epithelial cell subpopulations (BRCA1, NFE2L2 and STATs, etc) or affect prognosis (ATF3 and DDIT3) in ESCC were identified and maybe targets of future therapies, although more experiments are necessary to verify their significance.

Immunotherapy has revolutionized strategies in cancer treatment [62]. Within the therapeutic scenario, NK/T cell targeting therapies have become as potent and regenerate curative approaches for cancer patients with accurate targeting and strong efficacy [63]. Nevertheless, the strategy still undergoes manifold challenges, including immunosuppressive TME and depletion of neoplastic immune effector cells [64]. Based on above research background, we sought to explore the interactions between Epithelial cells and NK/T cells attempting to disclose underlying mechanism for immunotherapy resistance. Through CellChat analysis, we discovered several key ligand-receptor pairs in aforenoted two cell clusters. TIGIT, PDCD1 (PD1) and KLRB1 (NKRP1A) have been recognized as inhibitory receptor expressed in immune cells, such as activated T cells and NK cells [65–67]. Recent studies uncovered that TIGIT combines with ligands CD155 (PVR) and CD112 (PVRL2, nectin-2), which are expressed by cancer cells and antigen-presenting cell in the TME [68]. Anti-PD-1/PDL-1 has been a canonical case for immune checkpoint blockades (ICBs). When PD-1 binds to its ligand PD-L1, it generates inhibitory signals that inhibit the function of T cells, thereby preventing the immune system from attacking tumors. PD-1 and PD-L1 immunotherapy involves blocking the interaction between PD-1 and PD-L1 through anti PD-1 or anti PD-L1 antibodies, relieving the inhibition of T cells, and restoring their ability to attack tumors [69]. In our study, PVR-TIGIT and NECTIN2-TIGIT

pairs were also found as interactions between Epithelial cells and NK/T cells. The novel receptor ligand pairs (PDCD1LG2-PDCD1 and CLEC2B-KLRB1) provided a direction for ICBs. These results indirectly reveal that in the tumor microenvironment of ESCC, epithelial cells may influence the function of NK/T cells through ligand-receptor interactions, which in turn come to influence the immunoregulatory mechanisms in the tumor microenvironment.

It is worth noting that there are some limitations to our study. For example, the sample size of ESCC analyzed in this study is small, and the representativeness and robustness of the findings can be improved in the future by increasing the sample that includes different geographic regions and populations. In addition, despite our comprehensive analysis using bioinformatics tools, validation experiments in vitro and in vivo have not yet been performed by performing in vitro and in vivo validation experiments on key markers and ligand-receptor interactions. Finally, we will increase the depth and coverage of sequencing to capture more gene expression information. Advanced analytical methods such as spatial transcriptomics will also be employed to more comprehensively resolve cell-cell interactions and changes in the tumor microenvironment.

5. Conclusion

Collectively, our transcriptional map between ESCC and adjacent tissue offered a framework for comprehending the epithelial cell landscape. We explored differentiation trajectory of 4 epithelial cell subgroups in the development of ESCC. In addition, we revealed an important mechanism by which epithelial cells promote the development of ESCC through abnormal crosstalk between epithelial cells and NK/T cells. Our research findings may have far-reaching implications for understanding the tumor progression as well as for ESCC diagnosis and clinical treatment.

Ethics approval and consent to participate

Not applicable.

Financial disclosure

The study was supported by 900 Hospital Postdoctoral Fund.

Data availability statement

The datasets generated and/or analyzed during the current study are available in the [GSE196756] repository, [https://www.ncbi.nlm.nih.gov/geo/query/acc.cgi?acc= GSE196756]. And the code is available in https://github.com/whale-yjr/code-for-review.git.

Consent for publication

All authors have read and agreed to publish the article.

CRediT authorship contribution statement

Jingrong Yang: Writing – review & editing, Writing – original draft, Supervision, Software, Project administration, Methodology, Funding acquisition, Data curation, Conceptualization. **Bo Wu:** Writing – review & editing, Writing – original draft, Visualization, Software, Methodology, Formal analysis, Data curation, Conceptualization. **Guo Li:** Visualization, Supervision, Software, Project administration, Investigation. **Chenxi Zhang:** Visualization, Validation, Supervision, Resources, Methodology, Formal analysis. **Yongwei Xie:** Visualization, Validation, Supervision, Software, Project administration, Formal analysis. **Wencui Kong:** Writing – original draft, Visualization, Supervision, Resources, Methodology, Investigation. **Zhiyong Zeng:** Writing – review & editing, Supervision, Resources, Methodology, Formal analysis, Data curation.

Declaration of competing interest

The authors declare that they have no known competing financial interests or personal relationships that could have appeared to influence the work reported in this paper.

Acknowledgments

None.

Appendix A. Supplementary data

Supplementary data to this article can be found online at https://doi.org/10.1016/j.heliyon.2024.e38091.

Abbreviations

CNV copy number variation
ESCC esophageal squamous carcinoma
GEO Gene Expression Omnibus
GO Gene Ontology
PCA Principal Component Analysis
scRNA-seq single-cell RNA sequencing
TCGA The Cancer Genome Atlas
TLR3 Toll like receptor 3
TME tumor microenvironment
UMAP Uniform Manifold Approximation and Projection

References

[1] J. Zhan, W. Wang, Y. Tang, N. Zhou, D. Jiang, Development of a prognostic signature for esophageal cancer based on a novel 7-DNA damage repair genes signature, Biocell 46 (12) (2022) 2601–26013.
[2] L.-L. Lan, S.-H. Liu, Z.-T. Fan, X.-X. Wang, J.-T. Wang, K.-X. Wang, et al., SET domain containing protein 8 (SET8) promotes tumour progression and indicates poor prognosis in patients with laryngeal squamous cell carcinoma, Oncologie 25 (1) (2023) 61–69.
[3] W. Chen, R. Zheng, P.D. Baade, S. Zhang, H. Zeng, F. Bray, et al., Cancer statistics in China, 2015, CA: a cancer journal for clinicians 66 (2) (2016) 115–132.
[4] D. Zhao, Q. Wang, J. Wang, Mitochondrial autophagy gene signature predicts prognosis and response to immunity in esophageal cancer, Biocell 48 (2) (2024) 271–281.
[5] A. Pennathur, M.K. Gibson, B.A. Jobe, J.D. Luketich, Oesophageal carcinoma, Lancet. 381 (9864) (2013) 400–412.
[6] E.C. Smyth, V. Gambardella, A. Cervantes, T. Fleitas, Checkpoint inhibitors for gastroesophageal cancers: dissecting heterogeneity to better understand their role in first-line and adjuvant therapy, Ann. Oncol. : official journal of the European Society for Medical Oncology 32 (5) (2021) 590–599.
[7] M. Suntharalingam, K. Winter, D. Ilson, A.P. Dicker, L. Kachnic, A. Konski, et al., Effect of the addition of cetuximab to paclitaxel, cisplatin, and radiation therapy for patients with esophageal cancer: the NRG oncology RTOG 0436 phase 3 randomized clinical trial, JAMA Oncol. 3 (11) (2017) 1520–1528.
[8] P. van Hagen, M.C. Hulshof, J.J. van Lanschot, E.W. Steyerberg, M.I. van Berge Henegouwen, B.P. Wijnhoven, et al., Preoperative chemoradiotherapy for esophageal or junctional cancer, N. Engl. J. Med. 366 (22) (2012) 2074–2084.
[9] K.E. de Visser, J.A. Joyce, The evolving tumor microenvironment: from cancer initiation to metastatic outgrowth, Cancer Cell 41 (3) (2023) 374–403.
[10] L. Meng, Y. Zheng, H. Liu, D. Fan, The tumor microenvironment: a key player in multidrug resistance in cancer, Oncologie 26 (1) (2024) 41–58.
[11] X. Zhang, L. Peng, Y. Luo, S. Zhang, Y. Pu, Y. Chen, et al., Dissecting esophageal squamous-cell carcinoma ecosystem by single-cell transcriptomic analysis, Nat. Commun. 12 (1) (2021) 5291.
[12] Y. Chen, S. Zhu, T. Liu, S. Zhang, J. Lu, W. Fan, et al., Epithelial cells activate fibroblasts to promote esophageal cancer development, Cancer Cell 41 (5) (2023) 903, 18.e8.
[13] A. Zulibiya, J. Wen, H. Yu, X. Chen, L. Xu, X. Ma, et al., Single-cell RNA sequencing reveals potential for endothelial-to-mesenchymal transition in tetralogy of fallot, Congenit. Heart Dis. 18 (6) (2023) 611–625.
[14] Q. Ren, P. Zhang, X. Zhang, Y. Feng, L. Li, H. Lin, et al., A fibroblast-associated signature predicts prognosis and immunotherapy in esophageal squamous cell cancer, Front. Immunol. 14 (2023) 1199040.
[15] J. Zhou, G. Chen, J. Wang, B. Zhou, X. Sun, J. Wang, et al., Anti-PD-1 therapy achieves favorable outcomes in HBV-positive non-liver cancer, Oncogenesis 12 (1) (2023) 22.
[16] B. Zhou, W. Guo, L. Guo, Y. Li, Z. Zheng, Q. Huai, et al., Single-cell RNA-sequencing data reveals the genetic source of extracellular vesicles in esophageal squamous cell carcinoma, Pharmacol. Res. 192 (2023) 106800.
[17] K. Shi, Y. Li, L. Yang, Z. Zhang, D. Guo, J. Zhang, et al., Profiling transcriptional heterogeneity of epithelium, fibroblasts, and immune cells in esophageal squamous cell carcinoma by single-cell RNA sequencing, Faseb j 36 (11) (2022) e22620.
[18] T. Stuart, A. Butler, P. Hoffman, C. Hafemeister, E. Papalexi, W.M. Mauck 3rd, et al., Comprehensive integration of single-cell data, Cell 177 (7) (2019) 1888, 902.e21.
[19] F. Li, H. Wen, I. Bukhari, B. Liu, C. Guo, F. Ren, et al., Relationship between CNVs and immune cells infiltration in gastric tumor microenvironment, Front. Genet. 13 (2022) 869967.
[20] Y. Zheng, Z. Chen, Y. Han, L. Han, X. Zou, B. Zhou, et al., Immune suppressive landscape in the human esophageal squamous cell carcinoma microenvironment, Nat. Commun. 11 (1) (2020) 6268.
[21] S. Aibar, C.B. González-Blas, T. Moerman, V.A. Huynh-Thu, H. Imrichova, G. Hulselmans, et al., SCENIC: single-cell regulatory network inference and clustering, Nat. Methods 14 (11) (2017) 1083–1086.
[22] X. Qiu, Q. Mao, Y. Tang, L. Wang, R. Chawla, H.A. Pliner, et al., Reversed graph embedding resolves complex single-cell trajectories, Nat. Methods 14 (10) (2017) 979–982.
[23] S. Jin, C.F. Guerrero-Juarez, L. Zhang, I. Chang, R. Ramos, C.H. Kuan, et al., Inference and analysis of cell-cell communication using CellChat, Nat. Commun. 12 (1) (2021) 1088.
[24] W. Shen, Z. Song, X. Zhong, M. Huang, D. Shen, P. Gao, et al., Sangerbox: a comprehensive, interaction-friendly clinical bioinformatics analysis platform, iMeta 1 (3) (2022) e36.
[25] Y. Zhou, D. Yang, Q. Yang, X. Lv, W. Huang, Z. Zhou, et al., Single-cell RNA landscape of intratumoral heterogeneity and immunosuppressive microenvironment in advanced osteosarcoma, Nat. Commun. 11 (1) (2020) 6322.
[26] N.A. Winter, P.G. Gibson, V.M. McDonald, M. Fricker, Sputum gene expression reveals dysregulation of mast cells and basophils in eosinophilic COPD, Int J Chron Obstruct Pulmon Dis 16 (2021) 2165–2179.
[27] W. Kou, N. Zhao, L. Zhao, Z. Yin, M.C. Zhang, L. Zhang, et al., Single-cell characterization revealed hypoxia-induced metabolic reprogramming of gastric cancer, Heliyon 8 (11) (2022) e11866.
[28] I. Mattiola, A. Mantovani, M. Locati, The tetraspan MS4A family in homeostasis, immunity, and disease, Trends Immunol. 42 (9) (2021) 764–781.
[29] S. Wang, D. Lü, Z. Zhang, X. Jia, L. Yang, Effects of mechanical stretching on the morphology of extracellular polymers and the mRNA expression of collagens and small leucine-rich repeat proteoglycans in vaginal fibroblasts from women with pelvic organ prolapse, PLoS One 13 (4) (2018) e0193456.
[30] Q.L. Chen, L. Xia, S.P. Zhong, Q. Wang, J. Ding, X. Wang, Bioinformatic analysis identifies key transcriptome signatures in temporal lobe epilepsy, CNS Neurosci. Ther. 26 (12) (2020) 1266–1277.
[31] S.B. Kemp, N.G. Steele, E.S. Carpenter, K.L. Donahue, G.G. Bushnell, A.H. Morris, et al., Pancreatic cancer is marked by complement-high blood monocytes and tumor-associated macrophages, Life Sci. Alliance 4 (6) (2021).

[32] Y. Hong, L. Chen, J. Sun, L. Xing, Y. Yang, X. Jin, et al., Single-cell transcriptome profiling reveals heterogeneous neutrophils with prognostic values in sepsis, iScience 25 (11) (2022) 105301.
[33] J. Yang, S. Wu, W. Hu, D. Yang, J. Ma, Q. Cai, et al., Bmi1 signaling maintains the plasticity of airway epithelial progenitors in response to persistent silica exposures, Toxicology 470 (2022) 153152.
[34] F.A.R. da Silva, L.B. Pascoal, I. Dotti, M.L. Setsuko Ayrizono, D. Aguilar, B.L. Rodrigues, et al., Whole transcriptional analysis identifies markers of B, T and plasma cell signaling pathways in the mesenteric adipose tissue associated with Crohn's disease, J. Transl. Med. 18 (1) (2020) 44.
[35] M. Danoy, R. Jellali, Y. Tauran, J. Bruce, M. Leduc, F. Gilard, et al., Characterization of the proteome and metabolome of human liver sinusoidal endothelial-like cells derived from induced pluripotent stem cells, Differentiation 120 (2021) 28–35.
[36] D. Wen, X. Wang, R. Chen, H. Li, J. Zheng, W. Fu, et al., Single-cell RNA sequencing reveals the pathogenic relevance of intracranial atherosclerosis in blood blister-like aneurysms, Front. Immunol. 13 (2022) 927125.
[37] J. Yao, Q. Cui, W. Fan, Y. Ma, Y. Chen, T. Liu, et al., Single-cell transcriptomic analysis in a mouse model deciphers cell transition states in the multistep development of esophageal cancer, Nat. Commun. 11 (1) (2020) 3715.
[38] S.I. Fujii, K. Shimizu, Immune networks and therapeutic targeting of iNKT cells in cancer, Trends Immunol. 40 (11) (2019) 984–997.
[39] S. Xiao, G. Huang, W. Zeng, J. Zhou, Y. Li, T. Fan, et al., Roles of oncogenes in esophageal squamous cell carcinoma and their therapeutic potentials, Clin. Transl. Oncol. 25 (3) (2023) 578–591.
[40] W.J. Liu, Y. Zhao, X. Chen, M.L. Miao, R.Q. Zhang, Epigenetic modifications in esophageal cancer: an evolving biomarker, Front. Genet. 13 (2022) 1087479.
[41] M. Sheikh, G. Roshandel, V. McCormack, R. Malekzadeh, Current status and future prospects for esophageal cancer, Cancers 15 (3) (2023).
[42] A. Ooki, H. Osumi, K. Chin, M. Watanabe, K. Yamaguchi, Potent molecular-targeted therapies for advanced esophageal squamous cell carcinoma, Ther Adv Med Oncol 15 (2023) 17588359221138377.
[43] M.H. Shahrajabian, W.L. Sun, Survey on multi-omics, and multi-omics data analysis, integration and application, Cur. Phar. Ana. 19 (4) (2023) 267–281.
[44] J. Yang, X. Liu, S. Cao, X. Dong, S. Rao, K. Cai, Understanding esophageal cancer: the challenges and opportunities for the next decade, Front. Oncol. 10 (2020) 1727.
[45] J. Li, J. Xu, Y. Zheng, Y. Gao, S. He, H. Li, et al., Esophageal cancer: epidemiology, risk factors and screening, Chin. J. Cancer Res. 33 (5) (2021) 535–547.
[46] I.D. Nagtegaal, R.D. Odze, D. Klimstra, V. Paradis, M. Rugge, P. Schirmacher, et al., The 2019 WHO classification of tumours of the digestive system, Histopathology. 76 (2) (2020) 182–188.
[47] K. Schipper, A.P. Drenth, E. van der Burg, S. Cornelissen, S. Klarenbeek, M. Nethe, et al., Truncated ASPP2 drives initiation and progression of invasive lobular carcinoma via distinct mechanisms, Cancer Res. 80 (7) (2020) 1486–1497.
[48] Y. Liu, Y. Gu, Y. Han, Q. Zhang, Z. Jiang, X. Zhang, et al., Tumor exosomal RNAs promote lung pre-metastatic niche formation by activating alveolar epithelial TLR3 to recruit neutrophils, Cancer Cell 30 (2) (2016) 243–256.
[49] L. Bao, Z. Qian, M.B. Lyng, L. Wang, Y. Yu, T. Wang, et al., Coexisting genomic aberrations associated with lymph node metastasis in breast cancer, The Journal of clinical investigation 128 (6) (2018) 2310–2324.
[50] K. Xu, X. Zheng, H. Shi, J. Ou, H. Ding, MAD2L2, a key regulator in ovarian cancer and promoting tumor progression, Sci. Rep. 14 (1) (2024) 130.
[51] Y.E. Cho, J.H. Kim, Y.H. Che, Y.J. Kim, J.Y. Sung, Y.W. Kim, et al., Role of the WNT/β-catenin/ZKSCAN3 pathway in regulating chromosomal instability in colon cancer cell lines and tissues, Int. J. Mol. Sci. 23 (16) (2022).
[52] M.G. Diniz, F. Silva Jde, F.T. de Souza, N.B. Pereira, C.C. Gomes, R.S. Gomez, Association between cell cycle gene transcription and tumor size in oral squamous cell carcinoma, Tumour biology : the journal of the International Society for Oncodevelopmental Biology and Medicine 36 (12) (2015) 9717–9722.
[53] J. Folkman, Tumor angiogenesis: therapeutic implications, N. Engl. J. Med. 285 (21) (1971) 1182.
[54] R. Lugano, M. Ramachandran, A. Dimberg, Tumor angiogenesis: causes, consequences, challenges and opportunities, Cell. Mol. Life Sci. 77 (9) (2020) 1745–1770.
[55] A.J. Wiecek, D.H. Jacobson, W. Lason, M. Secrier, Pan-cancer survey of tumor mass dormancy and underlying mutational processes, Front. Cell Dev. Biol. 9 (2021) 698659.
[56] E.E. Wicks, G.L. Semenza, Hypoxia-inducible factors: cancer progression and clinical translation, J. Clin. Invest. 132 (11) (2022).
[57] Z. Miao, X. Zhao, X. Liu, Hypoxia induced β-catenin lactylation promotes the cell proliferation and stemness of colorectal cancer through the wnt signaling pathway, Exp. Cell Res. 422 (1) (2023) 113439.
[58] G. Hu, J. Ma, J. Zhang, Y. Chen, H. Liu, Y. Huang, et al., Hypoxia-induced lncHILAR promotes renal cancer metastasis via ceRNA for the miR-613/206/1-1-3p/Jagged-1/Notch/CXCR4 signaling pathway, Mol. Ther. 29 (10) (2021) 2979–2994.
[59] K.A. O'Brien, A.J. Murray, T.S. Simonson, Notch signaling and cross-talk in hypoxia: a candidate pathway for high-altitude adaptation, Life 12 (3) (2022).
[60] K. Ganesh, J. Massagué, Targeting metastatic cancer, Nat Med. 27 (1) (2021) 34–44.
[61] S. Gerstberger, Q. Jiang, K. Ganesh, Metastasis, Cell 186 (8) (2023) 1564–1579.
[62] Y. Zhang, Z. Zhang, The history and advances in cancer immunotherapy: understanding the characteristics of tumor-infiltrating immune cells and their therapeutic implications, Cell. Mol. Immunol. 17 (8) (2020) 807–821.
[63] O. Kyrysyuk, K.W. Wucherpfennig, Designing cancer immunotherapies that engage T cells and NK cells, Annu. Rev. Immunol. 41 (2023) 17–38.
[64] L. Zhi, X. Su, M. Yin, Z. Zhang, H. Lu, Z. Niu, et al., Genetical engineering for NK and T cell immunotherapy with CRISPR/Cas9 technology: implications and challenges, Cell. Immunol. 369 (2021) 104436.
[65] X. Yu, K. Harden, L.C. Gonzalez, M. Francesco, E. Chiang, B. Irving, et al., The surface protein TIGIT suppresses T cell activation by promoting the generation of mature immunoregulatory dendritic cells, Nat. Immunol. 10 (1) (2009) 48–57.
[66] K. Chamoto, T. Yaguchi, M. Tajima, T. Honjo, Insights from a 30-year journey: function, regulation and therapeutic modulation of PD1, Nat. Rev. Immunol. (2023).
[67] V.M. Braud, A. Meghraoui-Kheddar, R. Elaldi, L. Petti, C. Germain, F. Anjuère, LLT1-CD161 interaction in cancer: promises and challenges, Front. Immunol. 13 (2022) 847576.
[68] J.M. Chauvin, H.M. Zarour, TIGIT in cancer immunotherapy, J Immunother Cancer 8 (2) (2020).
[69] Y. Shiravand, F. Khodadadi, S.M.A. Kashani, S.R. Hosseini-Fard, S. Hosseini, H. Sadeghirad, et al., Immune checkpoint inhibitors in cancer therapy, Curr. Oncol. 29 (5) (2022) 3044–3060.